Modeling and Simulation of the Startup of a Pumped Storage Power Plant Unit

U. Karaagac, J. Mahseredjian, S. Dennetière

Abstract--**This paper presents the modeling and simulation study of the startup of a 250 MVA synchronous machine driven by a static frequency convertor (SFC) at a Pumped Storage Power Plant by utilizing EMTP-RV. The new synchronous machine (SM) module of EMTP-RV enables the simulation of the machine from standstill to rated speed, and therefore, makes it possible utilizing EMTP-RV for the electrical starting of pumped storage units. For the validation of the new SM module, the startup of an existing pumped storage power plant is simulated for the period from standstill to line operation including the synchronization of the machine to the grid. The simulation results and the field measurements demonstrate that the new SM module represents the machine behavior in a satisfying manner.**

Keywords: **pumped storage, EMTP-RV, synchronous machine**

I. INTRODUCTION

In pumped storage power plants, synchronous machines are operated as synchronous motors to pump the water from the lower reservoir to the upper reservoir and as synchronous generators to produce electrical power by using the falling energy of the water, which flows from the upper reservoir to the lower reservoir. This operation increases peak load capability and hence the power company can have ability to offer more electrical power to industries as well as households. The synchronous machines, therefore, need to be started and stopped frequently. Various systems have been proposed and implemented for the electrical starting of pumped storage units in the pumping mode. From the operation and economic point of views, utilizing static frequency convertors (SFC) has been demonstrated to be the more convenient in [1]. On the other hand, the operation of SFC generates disturbances in the voltage waveforms at the machine terminal and other connected equipments which should be analyzed in order to identify the potentially hazardous conditions, take the necessary preventive actions and/or design the required countermeasures for safe operation.

EMTP-RV [2] is an electromagnetic transients type program, which uses step-by-step numerical integration to solve the set of differential equations (linear and non-linear) representing the overall system under study. EMTP-RV allows detailed modeling of machines and system controllers as well as power electronic devices, circuit breaker actions, faults and other types of switching events. The new SM module of EMTP-RV enables simulating the machine from standstill to rated speed and therefore allows studying the startup of pumped storage units.

The actual Pumped Storage Power Plant (PSPP) is located in France and composed of four 250 MVA units for a total capacity of 1000 MVA. The SFC approach is utilized for electrical starting of units in the pumping mode. All manufacturer data regarding the existing synchronous machine and SFC was available for building the simulation model presented in this paper. In addition it was possible to access field measurements that included electrical frequency, field current, rms values of terminal voltages and currents and active and reactive powers delivered by the machine.

The provided manufacturer data regarding the SFC gives detailed information about the operating principle of the system. However, it does not include sufficient information in order to generate the mathematical model of the controller that can be directly utilized in the simulations. Therefore, an imitating controller with reasonable parameters is proposed for the simulations. The tuning study regarding the control parameters is performed on a simplified model in Simulink [3].

The complete system is simulated for the period from standstill to line operation including the synchronization of the machine to the grid. The simulation results and the field measurements show that the new SM module represents the machine behavior in a satisfying manner.

This paper consists of two main parts. In the first part, the system at the PSSP and the proposed simulation model, including the parameter tuning study, are presented. The new model and simulation results are discussed in the second part.

II. SYSTEM DESCRIPTION AND MODELLING

The simplified single line diagram of the PSPP is given in Fig. 1. At the pump storage station, there are four 250 MVA synchronous machines operating at 18 kV and each generator is connected to a 250 MVA, 18/400kV generator step-up (GSU) transformer. Two SFCs fed from the auxiliary bus of the station provide the source of variable voltage-variable frequency that supplies the synchronous machines during starting process in pumping mode.

Ulas Karaagac is with École Polytechnique de Montréal.
Jean Mahseredjian is with École Polytechnique de Montréal, Campus Université de Montréal, 2900, Édouard-Montpetit, Montréal (Québec), Canada, H3T 1J4 (corresponding author, 514-340-4711 (4870); e-mail: jeanm@polymtl.ca).
Sébastien Dennetière is with EDF Research and Development, France

Paper submitted to the International Conference on Power Systems Transients (IPST2009) in Kyoto, Japan June 3-6, 2009

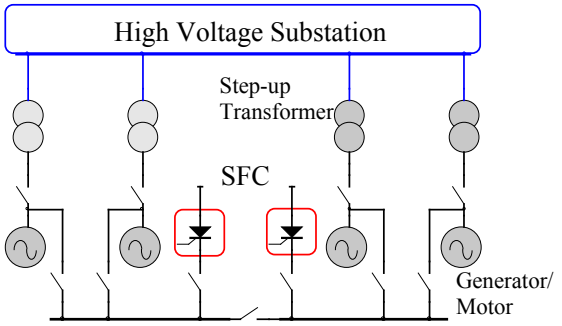

Fig. 1. Simplified one-line diagram of Pumped Storage Station

A. Static Frequency Convertor (SFC)

The SFC is basically composed of a rectifier bridge that converts the input from AC to DC and an inverter bridge that generates the variable frequency voltage from the DC stage. The inverter is configured as a current source inverter [4]. Fig. 2 shows the basic configuration of the static frequency converter. The switching sequence and output current relation is given in Table 1 where i_a, i_b and i_c are the machine line currents and I_{re} is the current at the DC interface of the SFC.

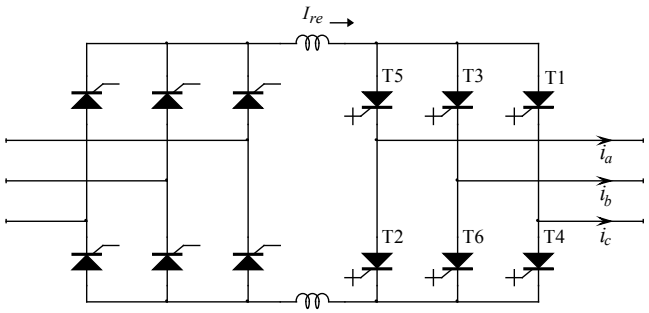

Fig. 2. Circuit model of the static frequency converter

Table 1. Switching sequence and output currents

Mode	mode1	mode2	mode3	mode4	mode5	mode6
Current	T6, T1	T1, T2	T2, T3	T3, T4	T4, T5	T5, T6
i_a	I_{re}	I_{re}	0	$-I_{re}$	$-I_{re}$	0
i_b	$-I_{re}$	0	I_{re}	I_{re}	I_{re}	$-I_{re}$
i_c	0	$-I_{re}$	$-I_{re}$	0	0	I_{re}

The currents produced by the SFC converter can be analyzed through Fourier decomposition:

$$i_a = \frac{2\sqrt{3}}{\pi} I_{re}\left(\cos\omega_e t - \frac{1}{5}\cos 5\omega_e t + \frac{1}{7}\cos 7\omega_e t + \ldots\right) \quad (1)$$

$$i_b = \frac{2\sqrt{3}}{\pi} I_{re}\left[\begin{array}{l}\cos\left(\omega_e t - \frac{2\pi}{3}\right) - \frac{1}{5}\cos\left(5\omega_e t + \frac{2\pi}{3}\right) \\ + \frac{1}{7}\cos\left(7\omega_e t - \frac{2\pi}{3}\right) + \ldots\end{array}\right] \quad (2)$$

$$i_c = \frac{2\sqrt{3}}{\pi} I_{re}\left[\begin{array}{l}\cos\left(\omega_e t + \frac{2\pi}{3}\right) - \frac{1}{5}\cos\left(5\omega_e t - \frac{2\pi}{3}\right) \\ + \frac{1}{7}\cos\left(7\omega_e t + \frac{2\pi}{3}\right) + \ldots\end{array}\right] \quad (3)$$

The inverter currents, given in equations (1) to (3), are converted to dq synchronous reference frame using Park's transformation [5]. After neglecting the harmonic components, the transformed inverter currents are written as follows:

$$\begin{bmatrix} i_d \\ i_q \\ i_o \end{bmatrix} = \begin{bmatrix} 0 \\ \frac{\sqrt{3}}{2\pi} I_{re} \\ 0 \end{bmatrix} \quad (4)$$

The d- and q- axis equivalent circuit representations of the synchronous machine are given in [6][7]. The electrical torque expression of the synchronous machine is given by:

$$T_e = \frac{3}{2}\frac{p}{2}\left[\begin{array}{l}\left(L_d\, i_d + L_{md}\, i'_{fd} + L_{md}\, i'_{dr}\right) i_q \\ -\left(L_q\, i_q + L_{mq}\, i'_{qr}\right) i_d\end{array}\right] \quad (5)$$

where p is the number of poles, L_d and L_q are the stator d and q-axis self inductances, L_{md} and L_{mq} are the d and q-axis mutual inductances, i'_{dr} and i'_{qr} are the d and q-axis rotor currents referred to the stator side and i'_{fd} is the field current referred to the stator side.

By considering only the fundamental component of the stator currents, i.e. neglecting harmonic components, the electrical torque expression of the synchronous machine can be written as:

$$T_e = \frac{3}{2}\frac{p}{2}\left(L_{md}\, i'_{fd} + L_{md}\, i'_{dr}\right) i_q \quad (6)$$

From (4) and (6), it can be concluded that it is possible to control the electrical torque of the machine by controlling the current I_{re} supplied by the rectifier.

B. SFC Control

The inverter is realized by utilizing gate turn-off controlled semiconductors (GTO), which can be forced to stop conduction from the control circuit. The control strategy of the inverter for synchronous machine starting is divided in two stages. The first stage requires forced commutation until 10% of the machine rated speed, the second stage uses natural commutation supported by the voltage induced in the machine windings.

The circuit layout and the control algorithm of the system are illustrated in Fig. 3 and Fig. 4 respectively (see [4] for more details). The control algorithm of the SFC is based on the rotor position, speed and terminal voltage. The inverter of the SFC is fired according to the position of the machine in order to follow the speed of the motor and the rectifier controls the magnitude of the current injected into the machine. The rectifier control is composed of two main control closed loops: an internal loop and an external loop. The internal loop is the current controller and it calculates the thyristor firing angle according to the reference and actual value of current. The external loop determines the torque control strategy by generating the current reference. It is composed of speed, frequency and angle controllers.

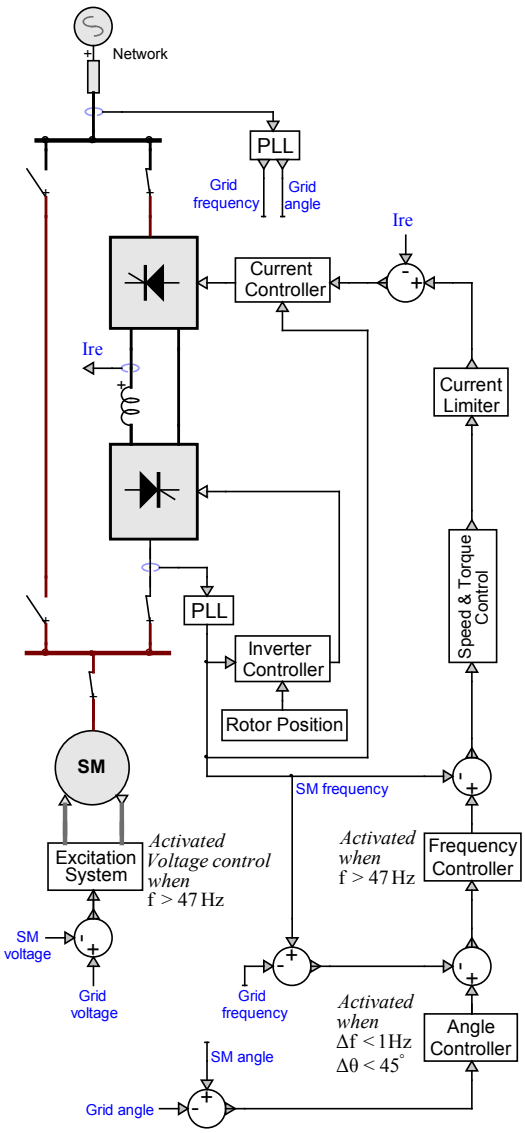

Fig. 3. Circuit layout for SFC fed synchronous motor drive

Forced Commutation Stage

The generated voltage by the machine rotating at low speeds is not sufficient to force the commutation of the thyristors in the inverter and hence, forced commutation is required. However, during forced commutation stage, when GTOs are forced to turn off, the overvoltage generated by the current source inductor at the DC interface might be very high and intolerable for the connected equipment. Therefore, the forced commutation stage includes a DC current cancellation mechanism, which is simply changing the operation mode of the rectifier to inverter. The cancellation of the current in the DC interface allows the commutation of the GTOs in the inverter and prevents the excessive overvoltage generated by the current source inductor at the DC interface.

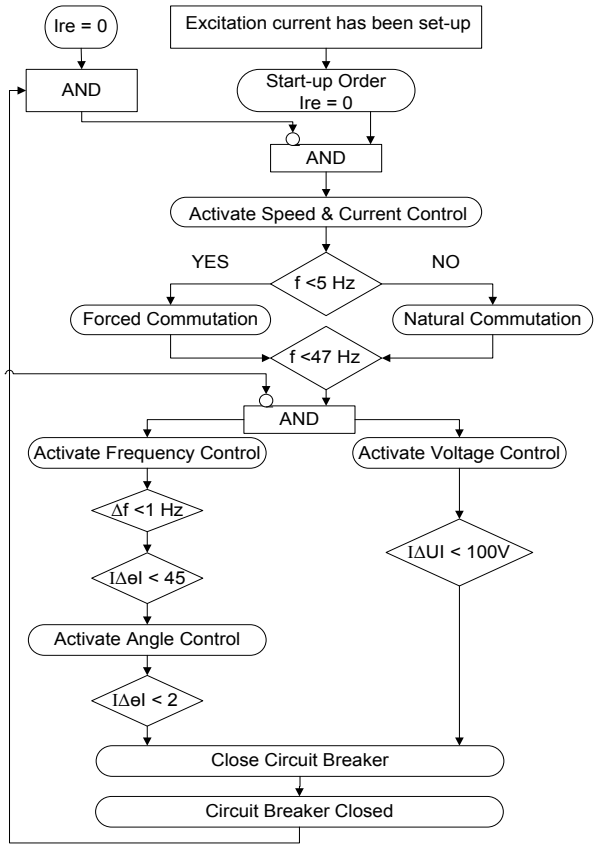

Fig. 4. Control algorithm of the system

Fig. 5 shows the firing sequence of the inverter bridge, and the theoretical waveforms of the currents in the SFC output while in the forced commutation stage. During each conduction period the current is interrupted by a time interval long enough to assure that the previously conducting thyristor in the inverter will not be re-ignited when the rectifier is re-started.

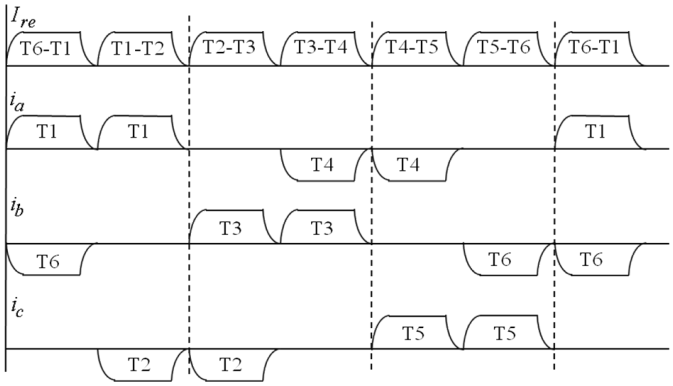

Fig. 5. Phase current waveforms and forced commutation sequence in the inverter bridge (i_a , i_b and i_c are the machine line currents, I_{re} is the current at the DC interface of the SFC)

Natural Commutation Stage

This stage uses natural commutation supported by the voltage induced in the machine windings. The speed controller provides acceleration of the machine up to 47 Hz with constant torque by keeping the DC current constant and hence the

corresponding AC currents of the machine constant. As the machine speed exceeds 47 Hz, the frequency controller is activated to bring the machine speed within the frequency margin needed for synchronization (fmach – fsys = +1Hz). Following the frequency controller, the angle controller is activated to bring the angle difference between the voltages of the system and the machine terminal within the margin required for synchronization.

The voltage controller is activated with the frequency controller i.e. when the machine speed exceeds 47 Hz. This controller brings the machine terminal voltage magnitude within the margin required for synchronization.

The manufacturer data provided in [4] does not include the parameters of the controllers. Therefore, the simplified model illustrated in Fig. 6 is simulated in Simulink and the parameters for speed, frequency and angle controllers are determined by a trial-and-error method. The Simulink simulation results of the system with the parameters utilized in EMTP-RV simulations are illustrated in Fig. 7 to Fig. 10.

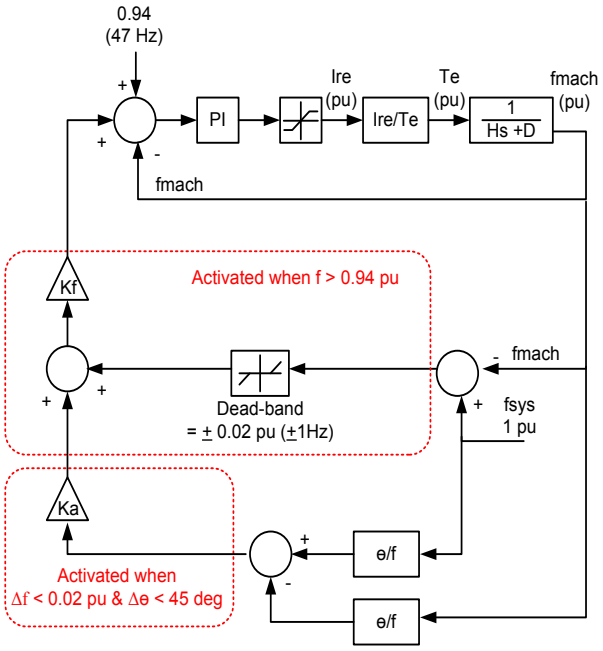

fmach : machine frequency
fsys : system frequency
Δf : abs(fsys – fmach)
Δθ : machine rotor position with respect to synchronously rotating frame (system)

Fig. 6. Simplified system model simulated in MATLAB/Simulink for controller parameter determination

The provided field measurement for frequency was obtained using the frequency meter of the SFC control system. This frequency meter takes the secondary side voltage of the voltage transformer which is connected to the generator terminal as input, and calculates frequency from the number of zero crossing points of the input voltage waveform. Although this frequency meter has a forth order low pass input filter with 100 Hz cut-off frequency, it measures frequency values which are different from the generator electrical speed during the forced commutation period (f < 5 Hz), due to the highly distorted voltage waveform at the measuring point. It can be seen from Fig. 7, that the frequency meter's accuracy range is above 6.4 Hz. The frequency controller of the SFC utilizes this frequency meter's output values as the frequency exceeds 47 Hz.

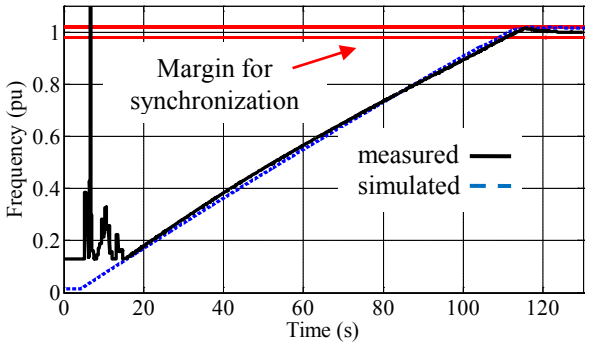

Fig. 7. Frequency measurement and simulation

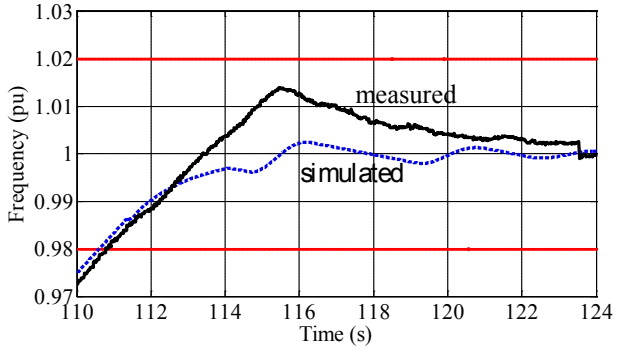

Fig. 8. Frequency measurement and simulation in the synchronization margin

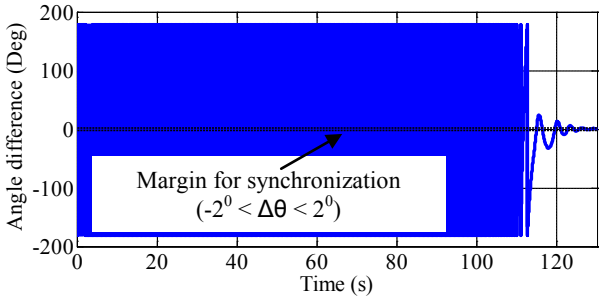

Fig. 9. Angle difference between the voltages of the generator terminal and the system

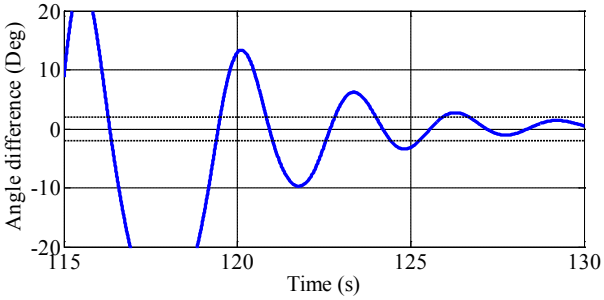

Fig. 10. Angle difference between the voltages of the generator terminal and the system in the synchronization margin

As shown in Fig. 8, with the proposed controller parameters, the rotor speed is expected to enter into the synchronization margin at about 111 s. Following frequency

controller, angle controller is initiated and the necessary condition for synchronization is expected to take place within a few seconds, as illustrated in Fig. 9 and Fig. 10.

C. Voltage Controller

The excitation system of the machine has an excitation field current controller which is active during electrical startup of the unit. The field current is kept constant at 1 pu until the machine electrical speed exceeds 47 Hz. The voltage controller is initiated when the machine speed exceeds 47 Hz and this controller brings the machine terminal voltage magnitude within the margin required for synchronization (100V) by changing the reference field current value (Ifref) of the field current controller of the excitation system. The block diagram of the voltage controller is given in Fig. 11.

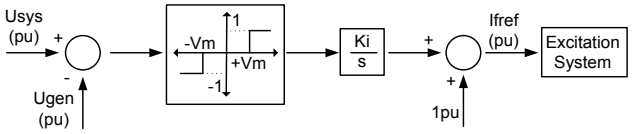

Fig. 11. Block diagram of the voltage controller, the blocks before to the left of the last summer are activated only when the frequency is higher than 0.94 pu

The voltage controller behavior of the system is different from the behavior stated in [4] as illustrated in Fig. 12. Although the voltage controller is expected to be activated as the frequency exceeds 0.94 pu (47 Hz), the measured values show that the voltage controller was initiated while the frequency was about 0.89 pu. Although the machine terminal voltage is below the upper synchronization voltage limit, the voltage controller reduces the field excitation current.

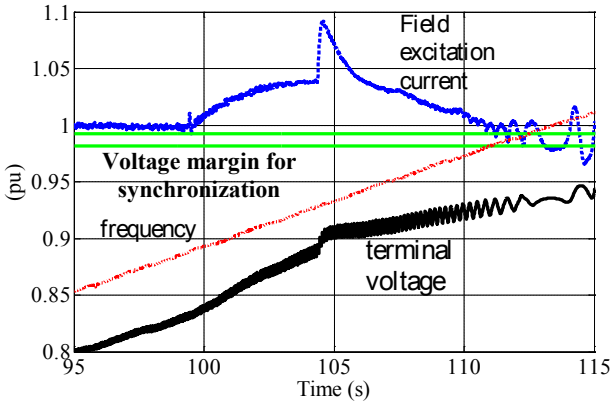

Fig. 12. Measured values: frequency, field excitation current and machine terminal voltage

D. New SM Module in EMTP-RV

In EMTP-RV, the synchronous machine is represented internally in dq0 coordinates, and interfaced with the external network using a Norton equivalent circuit in phase coordinates. A prediction-correction scheme is used for the machine variables, where the network variables can be solved with (optional) or without iterations. The readers should refer to [7] for more details.

EMTP-RV automatically initializes the machine equations using load-flow and steady-state solutions based on the system frequency, and therefore, does not allow starting the time-domain solution from machine standstill. In order to simulate the synchronous machine behavior during startup from zero Hz, it was required to implement a separate option where the electrical variables of the machine are initialized to zero and the mechanical variables of the machine are initialized based on zero mechanical speed.

III. SIMULATION RESULTS

A. Test system Model

The inverter side of the SFC is fully modeled by a six pulse bridge GTO inverter. Since the inverter is configured as a current source inverter in this application, the rectifier side is modeled as a controlled current source whose current value is determined by the external control loop including speed, frequency and angle controllers.

The synchronous machine is represented with its well-known dq0 equations and all necessary details. Typical values are used for the missing parameters regarding damper windings.

In order to represent the measuring circuit input filters, voltage and current transformer characteristics, typical lowpass filters are modeled at the measuring points.

The coupling circuit breaker is modeled by controlled switches which are activated when the synchronization conditions are satisfied.

B. Simulation Results

Since the voltage controller behavior of the system is different from the stated behavior given in [4], two different cases are simulated in this study. In Case-1 the voltage controller has the structure presented in [4]. In Case-2 the voltage controller generates a field current waveform similar to the provided measurements.

In both cases, the simulation time step is 100μs , the excitation field controller is activated at 0 s, the SFC is activated at 4.1 s and the total simulation time is 125 s. Simulation results and measured values are compared in the following figures.

The measured and simulated frequency plots are presented in Fig. 13 and zoomed on in Fig. 14. They demonstrate that the proposed controller model and parameters for the SFC representation can be considered to be acceptable to represent the behavior of the actual controller. The small difference between simulated and measured frequencies in the 6.4 Hz - 47 Hz frequency range is mainly due to the shaft model of the turbine. More accurate simulations can be obtained by using more accurate values of the inertia and speed damping constants of the turbine. However, the difference between the measured and simulated values becomes more apparent following the operation of frequency and angle controllers (starting at 47 Hz), which is expected according to the results obtained during the parameter tuning study performed with simplified Simulink model. More accurate modeling of the

SFC controller is expected to produce more accurate simulation results. However, this will require a parameter estimation study which may need additional tests and/or measurements on the SFC controller. It should be also noted that, after activation of the voltage controller, the field excitation is not constant and hence, the electrical torque changes not only under the control of the SFC controller, but also under the effect of the voltage controller.

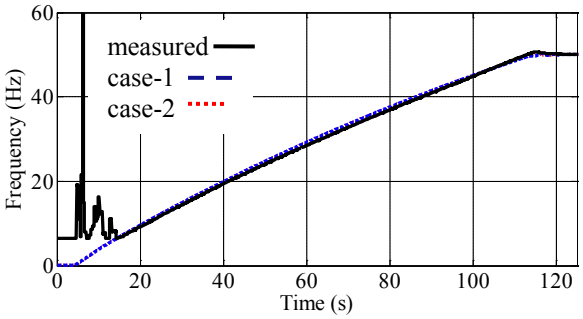

Fig. 13. Measured and simulated frequencies

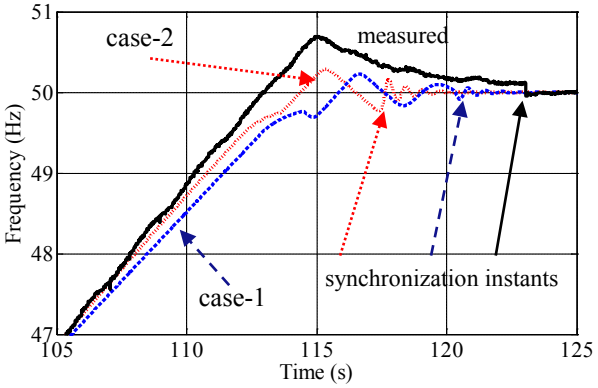

Fig. 14. Measured and simulated frequencies, zoomed version of Fig. 13

As seen from the machine field currents depicted in Fig. 15 and zoomed on in Fig. 16, the behavior of the voltage controller implemented for Case-2 is more accurate when compared to Case-1. The actual and the implemented voltage controller in Case-2 are activated before the voltage controller implemented in Case-1, resulting into higher machine field currents in the time interval from 98 s to 110 s, and hence, higher machine terminal voltage values as illustrated in Fig. 17 (zoomed in Fig. 18). Since the terminal voltage is small in Case-1 in this interval, the electrical power supplied to the machine is also small as illustrated in Fig. 19 and zoomed on in Fig. 20. It should be noted that the terminal voltage does not change only under the control of the voltage controller. Both the machine speed and the changes in machine stator currents supplied by the SCF affect the terminal voltage of the machine. The measured and simulated machine stator current plots are given in Fig. 21. The synchronization region is shown in Fig. 22. The simulation of Case-2 produces more accurate results due to more accurate representation of the effect of the voltage controller.

The simulation results demonstrate that the modified SM model is capable of representing startup from standstill. In addition to that, the proposed controller model and parameters for the SFC can be considered to be acceptable to represent the behavior of the actual controller.

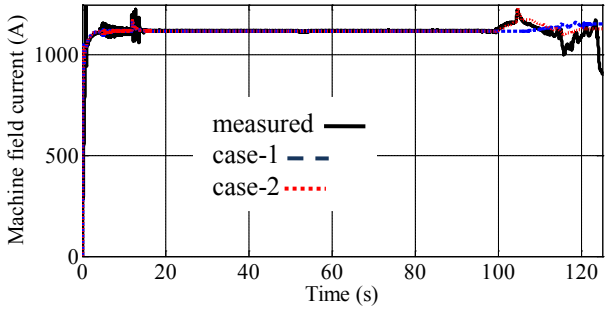

Fig. 15. Machine field currents

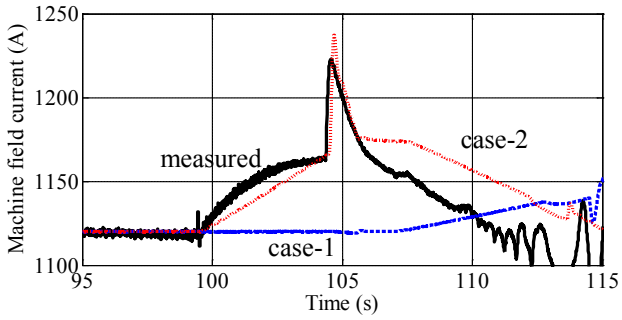

Fig. 16. Machine field currents, zoomed version of Fig. 15

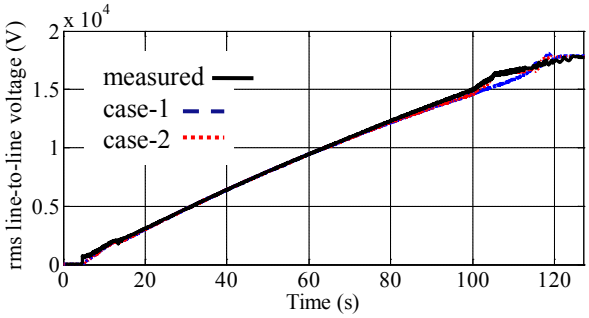

Fig. 17. Machine terminal rms line-to-line voltage

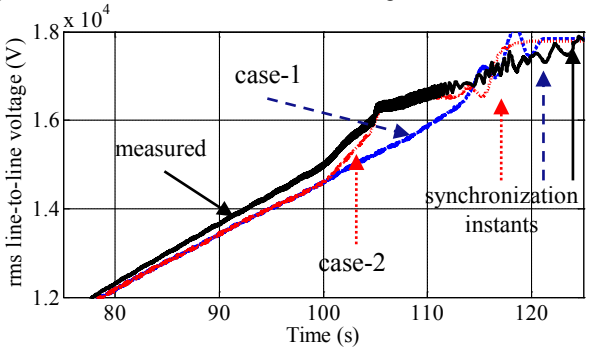

Fig. 18. Machine terminal rms line-to-line voltage, zoomed version of Fig. 17

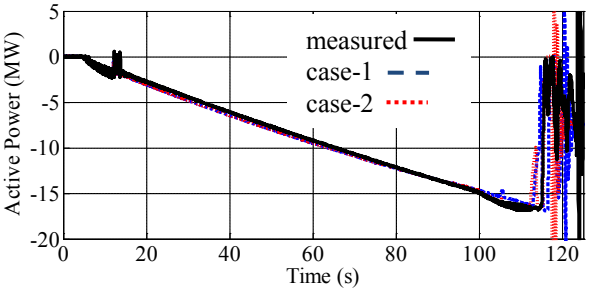

Fig. 19. Active power delivered by the machine

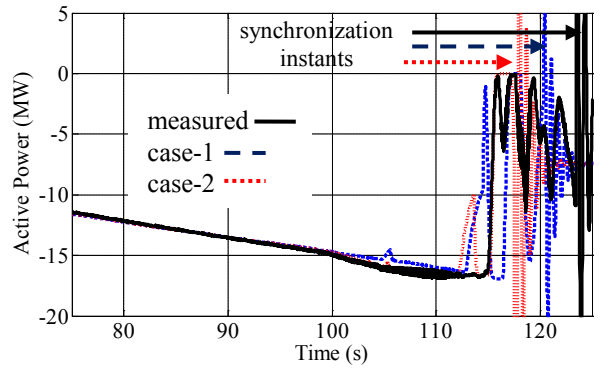

Fig. 20. Active power delivered by the machine, zoomed version of Fig. 19

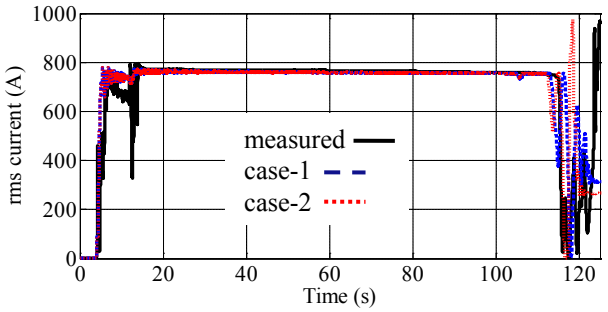

Fig. 21. Machine terminal rms current, phase a

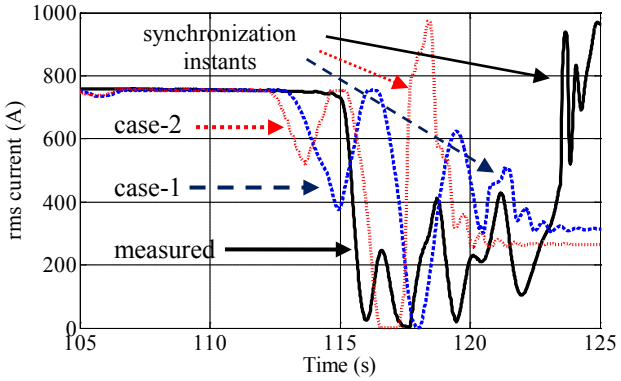

Fig. 22. Machine terminal rms current, phase a, zoomed version of Fig. 21

IV. CONCLUSIONS

This paper presented the modeling and simulation study of the startup of a 250 MVA synchronous machine driven by a static frequency convertor (SFC) at a Pumped Storage Power Plant. The simulation results and field measurements demonstrate that the modified synchronous machine model of EMTP-RV is capable to simulate synchronous machine behavior from standstill to rated speed conditions. Moreover, the proposed controller model and parameters for the SFC can be considered to be acceptable to represent the behavior of the actual controller. The proposed model of the system can be utilized to investigate the effects of disturbances in the voltage waveforms at the machine terminal and other connected equipments due to the operation of the SFC.

V. REFERENCES

[1] G. Magsaysay et al., “Use of a Static Frequency Converter for Rapid Load Response in Pumped-Storage Plants,” IEEE Trans. on Energy Conversion, Vol. 10, No. 4, December 1995.

[2] J. Mahseredjian, S. Dennetière, L. Dubé, B. Khodabakhchian and L. Gérin-Lajoie: “On a new approach for the simulation of transients in power systems”. Electric Power Systems Research, Volume 77, Issue 11, September 2007, pp. 1514-1520

[3] http://www.mathworks.com/

[4] L. Pierrat, J. Courault, "Système électronique de lancement d'alternateurs hydrauliques de pompage", Journées Parisiennes de la Société des Electriciens et Electroniciens (SEE), Paris, 14-16 Novembre 1984, (recueil des conférences SEE). Reproduction disponible: note EDF -DTG D4100 du 19-11-1984, 19 pages

[5] B. K. Bose, Power Electronics and AC Drives, Prentice-Hall, New Jersey, 1986

[6] S. P. Rosado “Analysis of Electric Disturbances from the Static Frequency Converter of a Pumped Storage Station” M.Sc. thesis, Virginia Polytechnic Institute and State University, Blacksburg, Virginia, 2001.

[7] J. Mahseredjian, EMTP-RV documentation, 2007.